High-moment corrections to the Drell-Yan cross section with an alternate parton density

Anibal Ramalho and George Sterman
Institute for Theoretical Physics, State University of New York at Stony Brook, Stony Brook, New York 11794
(Received 8 September 1983; revised manuscript received 13 February 1984)

We calculate order-α_s corrections to the Drell-Yan cross section $d\sigma/dQ^2$ using a previously defined alternate parton density. We find that the $\ln^2 n$ corrections to the nth moment of the cross section are absorbed into the process-independent density.

I. INTRODUCTION

Factorization theorems[1] play an important role in the analysis of hard hadron-hadron scattering. The classic form of factorization is for the Drell-Yan (DY) process at fixed invariant mass $Q^2 \equiv \tau S$ for the lepton pair. It is given by

$$\frac{d\sigma}{dQ^2} = \frac{4\pi\alpha^2}{9SQ^2} \sum_{a,b} \int_0^1 \frac{dx_1}{x_1} \frac{dx_2}{x_2} \theta(1-z) g_{1,a}(x_1,Q^2) \times \omega_{a,b}^{(g)}(z,Q^2) g_{2,b}(x_2,Q^2) , \quad (1.1)$$

where $z=\tau/x_1x_2$. The "parton density" $g_{i,a}(x_i,Q^2)$ is interpretable as the probability of finding parton a in hadron i with fraction x_i of that hadron's momentum. If the g's are chosen appropriately, the $\omega_{ab}^{(g)}(z,Q^2)$ are mass independent, and are short-distance-, ultraviolet- (UV) dominated functions. In an asymptotically free theory, they are thus in principle computable as an expansion in $\alpha_s(Q^2)$.

A standard choice for the g's is[2]

$$g_{i,a}(x,Q^2) = F_{i,a}(x,Q^2) , \quad (1.2)$$

where $F_{i,a}$ is the contribution of parton a to the relevant deep-inelastic-scattering (DIS) structure function of hadron i. The advantage of (1.2) is that $F_{i,a}$ is an experimental quantity which can be determined directly from DIS data. Equation (1.1) then directly specifies the normalization of the DY cross section, once $\omega^{(F)}$ is calculated as a power series in α_s.

The order-α_s corrections for $\omega^{(F)}$ have been calculated, but unfortunately they turn out to be too large to make the series for $\omega^{(F)}$ obviously convergent. The nature of these large corrections is most easily seen in terms of moments of the cross section with respect to $\tau=Q^2/S$. We have, for any choice of g,

$$\sigma(n,Q^2) \equiv \int_0^1 d\tau \tau^{n-1} (d\sigma/dQ^2) = \sum_{a,b} g_{1,a}(n,Q^2) \omega_{ab}^{(g)}(n,Q^2) g_{2,b}(n,Q^2) , \quad (1.3)$$

where $g(n,Q^2)$ and $\omega^{(g)}(n,Q^2)$ denote, respectively, moments of $g(x,Q^2)$ and $\omega^{(g)}(z,Q^2)$ with respect to x and z. Then[2,3] in order α_s,

$$\omega_{q\bar{q}}^{(F)}(n,Q^2) = \frac{\alpha_s(Q^2)}{2\pi} \tfrac{4}{3} [\xi(n) + 2\ln^2 n + \tfrac{4}{3}\pi^2] . \quad (1.4)$$

$\xi(n)$ is a bounded function of n which is much smaller than π^2. By itself, it gives a small correction. The π^2 term is associated with the difference between spacelike and timelike vertex corrections. It is present in $\sigma(n)$ but not in the $F(n,Q^2)$. $\ln^2 n$ terms, which are soft-gluon effects,[2,3,4] are found in both $\sigma(n)$ and the $F(n,Q^2)$, but with coefficients which do not match. Thus, terms of both types are left over in $\omega^{(F)}(n,Q^2)$. Various useful proposals have been made to resum these large corrections.[4,5] Here we offer a variant approach.

We use the fact that (1.2) is not the only possible choice for the $g_{i,a}(x,Q^2)$ in (1.1). Indeed, to systematically study certain semi-inclusive cross sections,[6] it has been necessary to introduce other parton densities.[6,7] Large-n moments are essentially semi-inclusive ($z\to 1$) cross sections themselves, and we shall consider a specific alternative choice,[7,8]

$$g(x,Q^2) = \phi(x,Q^2) , \quad (1.5)$$

with $\phi(x,Q^2)$ to be defined below. Our main result is that moments of $\phi(x,Q^2)$ absorb the leading $\ln^2 n$ terms in $\sigma(n,Q^2)$.

This result is analogous to the factorization of transverse-momentum dependence for the Drell-Yan cross section at low Q_T.[7,8] In fact, $\phi_{i,a}(x,Q^2)$ will be defined as an integral of the transverse-momentum-dependent parton densities encountered there. Our work thus suggests that the same formalism which is used to describe the DY cross section at low Q_T may also be applied to its large-n behavior.

The new densities ϕ are related to the DIS F's by the convolution[9]

$$\phi_{i,a}(x,Q^2) = \sum_c \int_x^1 \frac{dx'}{x'} C_{ac}\left[\frac{x}{x'},Q^2\right] F_{i,c}(x',Q^2) , \quad (1.6)$$

where the C_{ac} are UV-controlled "Wilson coefficient" functions, which can be computed as power series in $\alpha_s(Q^2)$. Using (1.1) and (1.6) we find the relation between the short-distance parts $\omega^{(F)}$ and $\omega^{(\phi)}$,

$$\omega_{ab}^{(F)} = \sum_{c,d} \int_0^1 \frac{dy_1}{y_1} \frac{dy_2}{y_2} C_{ad}(y_1) \omega_{cd}^{(\phi)}\left[\frac{z}{y_1y_2}\right] \times C_{db}(y_2) \theta\left[1-\frac{z}{y_1y_2}\right] . \quad (1.7)$$

Hence, if $\omega_{cd}^{(\phi)}$ is UV controlled, so will be $\omega_{ab}^{(F)}$. Argu-

ments for these results have been given in Ref. 10. From (1.6) and (1.7) we see that the normalization of $d\sigma/dQ^2$ in terms of $\phi_{i,a}$ is computable from the observable F's and the calculable functions $C_{ac}(x,Q^2)$. In this sense, the choices (1.2) and (1.5) are equivalent. (1.2) has the conceptual advantage of fixing the normalization of the DY cross section directly,[2,3] while we are claiming that (1.5) directly realizes a useful factorization for the semi-inclusive large-n cross section.

Before going into details, we can point out why the $\phi_{i,a}$ are appropriate densities, and how they differ from DIS structure functions. Leading $\ln^2 n$ terms come from regions where gluons are both soft and collinear to one or the other of the incoming hadrons (Sudakov regions). Now the $\phi_{i,a}$ are constructed to absorb all those contributions where gluons are collinear to hadron i, and to have *no other collinear enhancements.* Thus, Sudakov regions in the $\phi_{i,a}$ match those of the DY cross section. As we shall see, the DIS distributions $F_{i,a}(n,Q^2)$ include other collinear contributions in the $n\to\infty$ limit, which are not present in the original DY cross section. (This is related to the well-known differences in phase space between the two processes.[4,5]) By dividing $\sigma(n)$ by $F_{i,a}(n,Q^2)$ at large n, we effectively subtract out collinear contributions which are not there to begin with. This is one way to view the $\ln^2 n$ in Eq. (1.4).

To test these observations, we will compare $\omega^{(F)}(n,Q^2)$ of Eq. (1.4) with $\omega^{(\phi)}(n,Q^2)$ at order α_s. At this order we compute $\omega^{(\phi)}$ from Eq. (1.1) and a one-loop evaluation of $\phi(x,Q^2)$. $d\sigma/dQ^2$ is already given explicitly to one loop in Ref. 2, whose notation we follow. The factorization of all leading terms may be found by combining the one-loop result with standard soft-gluon arguments,[6,11] which we sketch only briefly.

The definition and graphical rules for $\phi_{i,a}$ are given in Sec. II, and Sec. III describes its calculation at one loop. In Sec. IV, we discuss factorization, and compute $\omega^{(F)}(n,Q^2)$. In Sec. V we trace the differences in $\omega^{(\phi)}$ and $\omega^{(F)}$ back to differences in the parton densities ϕ and F themselves.

II. DEFINITION OF THE ALTERNATE DENSITY

We will first briefly review the motivation for and the graphical construction of $\phi(x,Q^2)$. We then give its operator definition. Further details which pertain to the factorization of $\phi(x,Q^2)$ from cross sections and its computation will be found in Refs. 8 and 10.

Consider first the DY graphs represented in Fig. 1. In the $q^2/(p_i+p_j)^2\to 1$ limit, we find noncanceling leading contributions to $d\sigma/dQ^2$ when gluon momenta k^μ become parallel to either p_i^μ or p_j^μ and soft. A given k^μ, however soft, may be parallel to one or the other, but not both. This suggests the possibility that we can separate these leading contributions from each other. The densities $\phi_{i,q}$ are designed to do just this.

$\phi_{i,q}(x,Q^2)$ is defined, like the DIS structure functions, as a convolution of "bare" parton densities $q_0(x)$ and $G_0(x)$ with perturbative coefficients which describe their evolution. Thus, we write

$$\phi_{i,q}(z,Q^2)=\int_z^1 \frac{dx}{x}\left\{\left[\delta\left(1-\frac{z}{x}\right)+\frac{\alpha_s}{2\pi}r_{qq}\left(\frac{z}{x},Q^2\right)\right]q_0(x)+\frac{\alpha_s}{2\pi}r_{qG}\left(\frac{z}{x},Q^2\right)G_0(x)\right\}. \tag{2.1}$$

The perturbative part of $\phi_{i,q}$ is the sum of diagrams shown schematically in Fig. 2, which require the special Feynman rules for the double lines given in Fig. 3. The dotted line in Fig. 2 represents the integration and Dirac matrix

$$\tfrac{1}{2}\gamma^+\int d^4q'\,\delta(q'^+-xp^+)\,, \tag{2.2}$$

where q'^μ is the momentum flowing across the cut as shown. Dirac indices follow the dotted line, while group indices follow the eikonal lines.

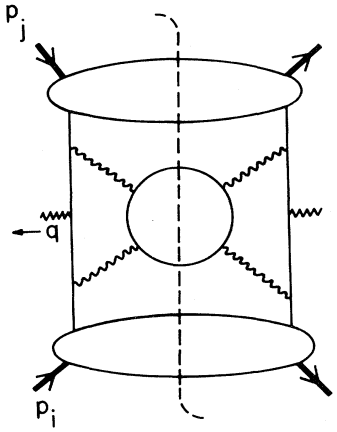

FIG. 1. Drell-Yan diagrams.

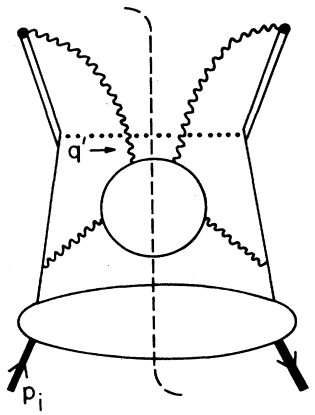

FIG. 2. Diagrams defining $\phi_{i,q}$.

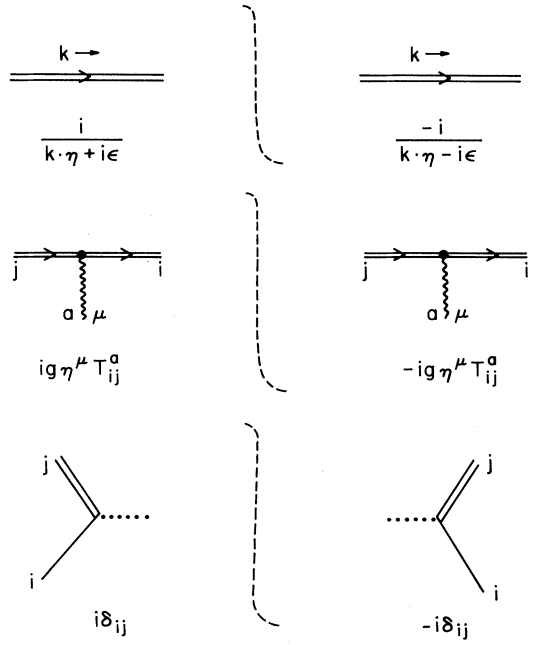

FIG. 3. Feynman rules for the parton density.

The double lines and corresponding vertices describe an eikonal line in the spacelike direction η^μ. The specific choices given below of η^μ and of the relative sign of the $i\epsilon$ are justified in detail in Ref. 7. The basic idea, however, is that the eikonal lines provide a good approximation to the effect of the opposite-moving incoming jet, as far as gluons collinear to p_i are concerned. When gluons which connect to the eikonal lines are not collinear to p_i, their contributions either are ultraviolet (and hence calculable) or cancel.[9]

Note that when we write $\phi_{i,q}(x,Q^2)$ we really mean

$$\phi_{i,q}\left[x,\frac{(p_i\cdot\eta)^2}{\eta^2}\right].$$

$\phi_{i,q}$ is frame dependent and we always work in the center of mass of the incoming system.

Precisely the same set of diagrams defines a distribution at fixed transverse momentum $\vec{k}_T$, by replacing (2.2) by

$$\tfrac{1}{2}\gamma^+\int d^4q'\delta(q'^+-xp^+)\delta^{(2)}(\vec{q}\,'_T-\vec{k}_T)\,. \tag{2.3}$$

If we call this distribution $P(x,\vec{k}_T,Q^2)$, then clearly

$$\phi(x,Q^2)=\int d\vec{k}_T P(x,\vec{k}_T,Q^2)\,. \tag{2.4}$$

The function $P(x,\vec{k}_T,Q^2)$ is used in studying the DY cross section at fixed muon-pair transverse momentum.[7,8]

By construction, $\phi_{i,q}(x,Q^2)$ includes leading contributions from regions where gluons are parallel to p_i^μ, but there are no additional lightlike vectors to generate collinear enhancements from other directions. We can contrast this to the DIS structure function $F_{i,q}$. When $x=-q^2/2q\cdot p_i\to 1$, the momentum of the hadronic final state is itself lightlike. This gives rise to new noncanceling collinear regions which have no counterpart in the DY cross section, Eq. (1.1) (see Sec. V).

The foregoing diagrams and rules may be defined in terms of operators as follows. We first define a quark operator $\psi_{\rm DY}$, with an eikonal line in η^μ direction attached, by

$$\psi_{\rm DY}(x^\nu)=O\exp\left[-ig\int_{-\infty}^{0}d\lambda\,\eta_\mu A_a^\mu(x^\nu+\lambda\eta^\nu)T^a\right]\psi(x^\nu)\,. \tag{2.5}$$

T^a are quark representation matrices, and O represents path ordering. It is straightforward to show that when $\psi_{\rm DY}$ is inserted into a matrix element it generates the eikonal lines and vertices shown in Fig. 3.

The distribution $\phi_{i,q}(x,Q^2)$ is then defined by

$$\phi_{i,q}\left[x,\frac{(\eta\cdot p_i)^2}{\eta^2}\right]=\frac{1}{2(2\pi)}\int dy^-e^{-ixp_i^+y^-}\langle p_i\,|\,\bar{\psi}_{\rm DY}(0,y^-,\vec{0}_T)\gamma^+\psi_{\rm DY}(0)\,|\,p_i\rangle\,. \tag{2.6}$$

Similarly, the distribution at fixed transverse momentum is

$$P_{i,q}\left[x,\vec{k}_T,\frac{(\eta\cdot p_i)^2}{\eta^2}\right]=\frac{1}{2(2\pi)^3}\int dy^-d\vec{y}_T e^{-i(xp_i^+y^--\vec{k}_T\cdot\vec{y}_T)}\langle p_i\,|\,\bar{\psi}_{\rm DY}(0,y^-,\vec{y}_T)\gamma^+\psi_{\rm DY}(0)\,|\,p_i\rangle\,. \tag{2.7}$$

These definitions clearly satisfy the relation (2.4).

III. ONE-LOOP CALCULATION

The order-α_s graphs which contribute to the perturbative density functions r_{qq} and r_{qG} of Eq. (2.1) are shown in Figs. 4 and 5, respectively. We ignore eikonal-eikonal interactions, which are unphysical and do not contribute to the n dependence. We have left the dotted lines out of the pictures, but the Feynman rules are as described in Sec. II.

Quark masses are set to zero throughout the calcula-

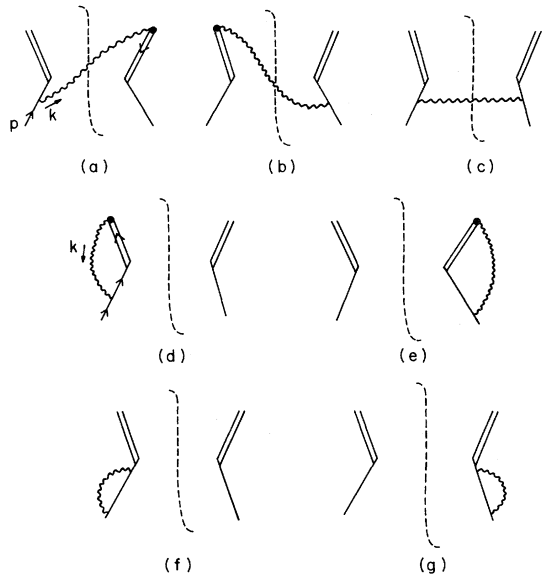

FIG. 4. Quark graphs that contribute to the parton density.

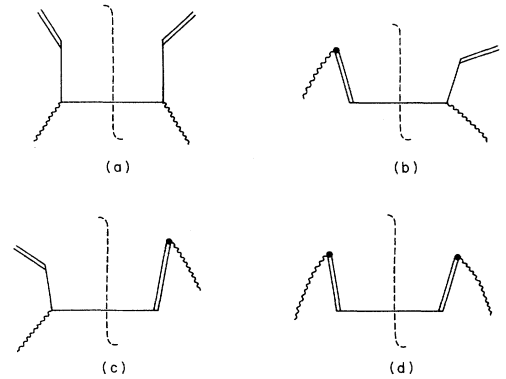

FIG. 5. Gluon graphs that contribute to the parton density.

tions, and external lines are set on-shell.[11] Loop integrals give rise to ultraviolet and infrared divergences (including mass singularities). Both are regulated dimensionally, and ultraviolet divergences are removed by minimal subtraction.

The distributions under discussion are gauge invariant, and for the sake of simplicity, we use the Feynman gauge. The direction of the eikonal line is specified by a spacelike vector $\eta^\mu=(\eta^+,\eta^-,\vec{\eta}_T)$, with $\eta^+<0$, $\eta^->0$, and $|\eta^+/\eta^-|=O(1)$.[7] Here, as usual, one defines the light-cone variables

$$\eta^\pm\equiv\frac{1}{\sqrt{2}}(\eta^0\pm\eta^3)\ .$$

It is convenient to consider the initial-state parton momenta along the z axis. Thus, we choose $\eta^\mu=(-1,1,\vec{0}_T)$ and the momentum of the incoming quark (or gluon) as

$$p^\mu=((s/2)^{1/2},0,\vec{0}_T)\ ,$$

where s is the parton center-of-mass energy, assumed large.

Now let us examine graphs 4(a) and 4(d) in some detail, in order to show a few technical points involved in our analysis. When spin and color averaged, diagram 4(a) reads

$$\frac{\alpha_s}{2\pi}r_{qq}^{4(a)}(z)=+\tfrac{1}{4}\tfrac{4}{3}g^2\mu^{4-n}\int\frac{d^nk}{(2\pi)^n}\frac{tr[\not p\gamma^+(\not p-\not k)\not\eta]}{[(p-k)^2+i\epsilon](-k\cdot\eta-i\epsilon)}2\pi\delta_+(k^2)\delta(k^+-(1-z)p^+)\ , \tag{3.1}$$

where z is the fraction of the incoming parton momentum flowing along the internal fermion line, and we drop the explicit Q dependence in r. The integrations over k^+ and k^- are straightforward and the expression reduces to the following:

$$\frac{\alpha_s}{2\pi}r_{qq}^{4(a)}(z)=-2z(1-z)s\tfrac{4}{3}\alpha_s\mu^{4-n}\times\int\frac{d^{n-2}k_T}{(2\pi)^{n-2}}\frac{1}{\vec{k}_T^{\,2}[\vec{k}_T^{\,2}-(1-z)^2s]}\ . \tag{3.2}$$

The integral is defined over Euclidean space in $n-2$ dimensions. The result is

$$r_{qq}^{4(a)}(z)=-\frac{1}{\epsilon}\frac{4}{3}\left[-\frac{4\pi\mu^2}{s}\right]^\epsilon\Gamma(1+\epsilon)z(1-z)^{-1-2\epsilon}\ , \tag{3.3}$$

where $\epsilon\equiv2-n/2$. It is interesting to find the factor $(-1)^\epsilon$ present in the result, since in discussing graph 4(a), one is dealing with real emission. This is due to the presence of the eikonal denominator in (3.1). Usually such a factor comes from the analytic continuation of the vertex correction from spacelike (deep-inelastic scattering) to timelike (Drell-Yan) q^2. When expanded to second order in ϵ and multiplied by the term which contains the double logarithms, it gives rise to most of the so-called π^2 corrections. The term $(1-z)^{-1-2\epsilon}$ is evidently infrared singular. Using the identity[2]

$$z^\epsilon(1-z)^{-1-\epsilon}=-\frac{1}{\epsilon}\delta(1-z)+\frac{1}{(1-z)_+}-\epsilon\left[\frac{\ln(1-z)}{1-z}\right]_++\epsilon\frac{\ln z}{1-z}+O(\epsilon^2)\ , \tag{3.4}$$

we can rewrite $r_{qq}^{4(a)}(z)$ as

$$r_{qq}^{4(a)}(z)=\tfrac{1}{2}\tfrac{4}{3}\left[\frac{4\pi\mu^2}{s}\right]^{\epsilon}\frac{\Gamma(1-\epsilon)}{\Gamma(1-2\epsilon)}\left[\frac{1}{\epsilon^2}\delta(1-z)-\frac{2}{\epsilon}\frac{z}{(1-z)_+}+4z\left[\frac{\ln(1-z)}{1-z}\right]_+-\frac{\pi^2}{6}\delta(1-z)+O(\epsilon)\right]. \tag{3.5}$$

Nowhere are purely imaginary terms shown explicitly, since they eventually cancel when the contributions from each graph and its complex conjugate are put together. As usual, all distributions $D_+(z)$, with a + prescription, are defined in such a way that, for any test function $f(z)$, sufficiently regular at the end points,

$$\int_0^1 dz\, f(z)D_+(z)=\int_0^1 dz\, D(z)[f(z)-f(1)]\,. \tag{3.6}$$

Now consider the virtual graph 4(d):

$$\frac{\alpha_s}{2\pi}r_{qq}^{4(d)}(z)=\frac{+i}{4p^+}\delta(1-z)\tfrac{4}{3}g^2\mu^{4-n}\times\int\frac{d^nk}{(2\pi)^n}\frac{tr[\not p\gamma^+(\not p+\not k)\not\eta]}{(-k\cdot\eta+i\epsilon)(k^2+i\epsilon)[(p+k)^2+i\epsilon]}. \tag{3.7}$$

On integration, (3.7) yields

$$r_{qq}^{4(d)}(z)=r_{IR}^{4(d)}(z)+r_{UV}^{4((d)}(z)\,, \tag{3.8}$$

$$r_{IR}^{4(d)}(z)=\delta(1-z)\frac{4}{3}\left[-\frac{4\pi\mu^2}{s}\right]^{\epsilon}\Gamma(1+2\epsilon)\times\left[-\frac{\Gamma(-2\epsilon)\Gamma(-\epsilon)}{\Gamma(1-2\epsilon)}+\frac{\Gamma(-\epsilon)}{1-2\epsilon}\right], \tag{3.9}$$

$$r_{UV}^{4(d)}(z)=\delta(1-z)\frac{4}{3}\left[-\frac{4\pi\mu^2}{s}\right]^{\epsilon}\frac{\Gamma(1-\epsilon)}{1-2\epsilon}\Gamma(2\epsilon)\,. \tag{3.10}$$

The ultraviolet and infrared divergences present in the integral of Eq. (3.7) are manifest in $r_{UV}^{4(d)}(z)$ and $r_{IR}^{4(d)}(z)$, respectively. The regions of definition of these two quantities in the variable ϵ are clearly disjoint, and $r_{UV}^{4(d)}(z)$ and $r_{IR}^{4(d)}(z)$ must be treated separately. Once the ultraviolet divergences have been removed, the sum of the diagrams is well defined for $n>4$. The ultraviolet pole of $r_{UV}^{4(d)}(z)$ is extracted by minimal subtraction:

$$r_{UV}^{4(d)}(z)-(\text{UV pole})=\tfrac{1}{2}\tfrac{4}{3}(2+\ln 4\pi-\gamma_E)\delta(1-z)\,. \tag{3.11}$$

Notice that the factor $(-1)^{\epsilon}$ occurs in $r^{4(d)}(z)$ as well. Since $r_{IR}^{4(d)}(z)$ contains a double pole, we are bound to get further π^2 terms. Indeed, $r_{qq}^{4(d)}(z)$ is found to be of the form

$$r_{qq}^{4(d)}(z)=\tfrac{1}{2}\tfrac{4}{3}\left[\frac{4\pi\mu^2}{s}\right]^{\epsilon}\frac{\Gamma(1-\epsilon)}{\Gamma(1-2\epsilon)}\delta(1-z)\left[-\frac{1}{\epsilon^2}-\frac{2}{\epsilon}-2-\frac{\pi^2}{6}+\ln 4\pi-\gamma_E+O(\epsilon)\right]. \tag{3.12}$$

There is a neat cancellation of the double poles when we add the contributions from $r^{4(a)}(z)$ and $r^{4(d)}(z)$. This is the Bloch-Nordsieck mechanism of cancellation of soft singularities at work.

The computation of the remaining diagrams follows in a similar fashion. Figure 5 shows all the relevant diagrams with a gluon in the initial state. However, if the average over the polarizations of the gluon includes only the physical states, then graphs 5(b), 5(c), and 5(d) vanish identically. This follows trivially from the fact that any transverse polarization of the incoming gluon ought to be orthogonal to the vector η^{μ} specifying the direction of the eikonal line. Thus, all the contribution arises from Fig. 5(a), suggesting a nice parton-model interpretation.

We can summarize the complete result of the one-loop calculations of r_{qq} and r_{qG} as follows. Defining $t=-1/\epsilon$ and choosing $\mu^2=s$, we have

$$\begin{aligned} r_{qq}(z,Q^2)&=tP_{qq}(z)+\rho_{qq}(z)\,,\\ r_{qG}(z,Q^2)&=tP_{qG}(z)+\rho_{qG}(z)\,, \end{aligned} \tag{3.13}$$

where the ρ's are ϵ independent. The functions P_{qq} and P_{qG} are the standard QCD evolution coefficients,[12]

$$\begin{aligned} P_{qq}(x)&=\frac{4}{3}\left[\frac{1+x^2}{(1-x)_+}+\tfrac{3}{2}\delta(1-x)\right],\\ P_{qG}(x)&=\tfrac{1}{2}[x^2+(1-x)^2]\,. \end{aligned} \tag{3.14}$$

The contributions of each graph to ρ_{qq} and ρ_{qG} are given in Table I. Their sums are

$$\begin{aligned} \rho_{qq}(z)=\frac{4}{3}\Bigg[&2(1+z^2)\left[\frac{\ln(1-z)}{1-z}\right]_+-2(1-z)\ln(1-z)-\tfrac{1}{2}(4+\tfrac{2}{3}\pi^2-\ln 4\pi+\gamma_E)\delta(1-z)\\ &+(\ln 4\pi-\gamma_E)(1-z)-(\ln 4\pi-\gamma_E)\left[\frac{1+z^2}{(1-z)_+}+\frac{3}{2}\delta(1-z)\right]\Bigg],\\ \rho_{qG}(z)=0\,. \end{aligned} \tag{3.15}$$

TABLE I. Individual contributions of the diagrams in Figs. 4 and 5 to the quantities ρ_{qq} and ρ_{qG}.

$\rho_{qq}^{4(a)}=\rho_{qq}^{4(b)}=$	$\frac{4}{3}\left[2z\left[\frac{\ln(1-z)}{1-z}\right]_+-\frac{\pi^2}{12}\delta(1-z)-\frac{z}{(1-z)_+}(\ln 4\pi-\gamma_E)\right]$
$\rho_{qq}^{4(d)}=\rho_{qq}^{4(e)}=$	$-\frac{4}{3}\left[1+\frac{\pi^2}{12}+\frac{1}{2}(\ln 4\pi-\gamma_E)\right]\delta(1-z)$
$\rho_{qq}^{4(c)}=\rho_{qq}^{4(f)}=\rho_{qq}^{4(g)}=$	0
$\rho_{qG}^{5(a)}=\rho_{qG}^{5(b)}=\rho_{qG}^{5(c)}=\rho_{qG}^{5(d)}=$	0

We have put ρ_{qq} into this form for ease of comparison below. Finally, we note that many ρ's are zero because the corresponding graphs formally vanish in dimensional regularization and are only nonzero because of the minimal UV subtraction.

IV. FACTORIZATION AND MOMENTS

In this section, we discuss factorization with the parton density $\phi(x,Q^2)$. Using results of Sec. III, we compute the one-loop corrections in the short-distance function $\omega_{q\bar{q}}^{(\phi)}$. We take moments and compare to the corresponding function $\omega_{q\bar{q}}^{(F)}$, found by factoring the DIS structure functions.[2,3]

Radiative corrections to the short-distance functions $\omega_{q\bar{q}}$ are calculated by expanding both sides of Eq. (1.1). To order α_s, the left-hand side is given by[2] (for one quark flavor of charge e_q),

$$\frac{d\sigma}{dQ^2}=\frac{4\pi\alpha^2}{9SQ^2}e_q^2\int_0^1\frac{dx_1}{x_1}\int_0^1\frac{dx_2}{x_2}\left\{[q_0^{(1)}(x_1)\bar{q}_0^{(2)}(x_2)+(1\leftrightarrow 2)]\left[\delta(1-z)+\theta(1-z)\left[\frac{\alpha_s}{2\pi}2P_{qq}(z)t+\alpha_s f_{q,\mathrm{DY}}(z)\right]\right]\right.$$
$$\left.+\{[q_0^{(1)}(x_1)+\bar{q}_0^{(1)}(x_1)]G_0^{(2)}(x_2)+(1\leftrightarrow 2)\}\theta(1-z)\left[\frac{\alpha_s}{2\pi}P_{qG}(z)t+\alpha_s f_{G,\mathrm{DY}}(z)\right]\right\}. \tag{4.1}$$

The functions P_{qq} and P_{qG} are given in Eq. (3.14), and[2]

$$\alpha_s f_{q,\mathrm{DY}}(z)=\frac{\alpha_s(Q^2)}{2\pi}\frac{4}{3}\left[4(1+z^2)\left[\frac{\ln(1-z)}{1-z}\right]_+-2\frac{1+z^2}{1-z}\ln z+(\tfrac{2}{3}\pi^2-8)\delta(1-z)\right.$$
$$\left.-2\left[\frac{1+z^2}{(1-z)_+}+\tfrac{3}{2}\delta(1-z)\right](\ln 4\pi-\gamma_\epsilon)\right], \tag{4.2a}$$

$$\alpha_s f_{G,\mathrm{DY}}(z)=\frac{\alpha_s(Q^2)}{2\pi}\frac{1}{2}\left[[z^2+(1-z)^2]\ln\frac{(1-z)^2}{z}-\tfrac{3}{2}z^2+z+\tfrac{3}{2}-[z^2+(1-z)^2](\ln 4\pi-\gamma_E)\right]. \tag{4.2b}$$

Note that Ref. 2 uses $\mu^2=Q^2$, whereas we take $\mu^2=s$. This makes a slight difference in the finite part given below. The expansion of the densities $g=\phi$ on the right-hand side of (1.1) is given by Eq. (2.1). Finally, we expand $\omega_{q\bar{q}}^{(\phi)}$ to one loop by

$$\omega_{q\bar{q}}^{(\phi)}(z)=e_q^2\left[\delta(1-z)+\frac{\alpha_s}{2\pi}\omega_{q\bar{q}}^{(\phi,1)}(z)\right],$$
$$\omega_{qG}^{(\phi)}(z)=e_q^2\frac{\alpha_s}{2\pi}\omega_{qG}^{(\phi,1)}(z). \tag{4.3}$$

This gives, for the right-hand side of (1.1),

$$\frac{4\pi\alpha^2}{9SQ^2}e_q^2\int_0^1\frac{dx_1}{x_1}\int_0^1\frac{dx_2}{x_2}\left[[q_0^{(1)}(x_1)\bar{q}_0^{(2)}(x_2)+(1\leftrightarrow 2)]\left[\delta(1-z)+\theta(1-z)\frac{\alpha_s}{2\pi}[\omega_{q\bar{q}}^{(\phi,1)}(z)+2r_{qq}(z)]\right]\right.$$
$$\left.+\left[[q_0^{(1)}(x_1)+\bar{q}_0^{(1)}(x_1)]G_0^{(2)}(x_2)+(1\leftrightarrow 2)\right]\theta(1-z)\frac{\alpha_s}{2\pi}[\omega_{qG}^{(\phi,1)}(z)+r_{qG}(z)]\right]. \tag{4.4}$$

Finally, using Eqs. (3.13) to (3.15) and comparing Eqs. (4.1) and (4.4), we find

$$\begin{aligned}\omega_{q\bar{q}}^{(\phi,1)}(z)&=2\pi f_{q,\mathrm{DY}}(z)-2\rho_{qq}(z)\\&=\tfrac{4}{3}[4(1-z)\ln(1-z)-2(\ln 4\pi-\gamma_E)(1-z)+(\tfrac{4}{3}\pi^2-4-\ln 4\pi+\gamma_E)\delta(1-z)]\,,\\\omega_{qG}^{(\phi,1)}(z)&=2\pi f_{G,\mathrm{DY}}(z)-\rho_{qG}(z)\\&=\tfrac{1}{2}\{[z^2+(1-z)^2][2\ln(1-z)-\ln 4\pi+\gamma_E]-\tfrac{3}{2}z^2+z+\tfrac{3}{2}\}\,.\end{aligned}\tag{4.5}$$

This is the basic result of our calculation. We first note that the $P_{qq}t$ and $P_{qG}t$ terms are absent in the short-distance parts $\omega_{q\bar{q}}^{(\phi,1)}$ and $\omega_{qG}^{(\phi,1)}$. This is equivalent to one-loop factorization for the $\phi_{i,a'}$ since the explicit Q^2 dependence due to parton evolution has been absorbed into the parton distributions. This, of course, is also true when the DIS structure functions are factored out. What is new here is that the terms $[\ln(1-z)/(1-z)]_+$ in $f_{q,\mathrm{DY}}$ have also been absorbed into the $\phi_{i,q}$ [see Eq. (3.15)], and are hence absent from the $\omega_{ab}^{(\phi,1)}$. The consequences of this difference are best seen in terms of moments.

The moments of Eq. (4.5) are given by

$$\omega_{q\bar{q}}^{(\phi,1)}(n)=\tfrac{4}{3}\left[\frac{4}{(n+1)^2}-\frac{4}{n(n+1)}\sum_{j=1}^{n}\frac{1}{j}-\left[1+\frac{2}{n(n+1)}\right](\ln 4\pi-\gamma_E)+\tfrac{4}{3}\pi^2-4\right],\tag{4.6}$$

$$\omega_{qG}^{(\phi,1)}(n)=\frac{1}{2}\left[\frac{4}{(n+1)^2}-\frac{4}{(n+1)(n+2)}-\frac{4}{(n+2)^2}-\frac{n^2+n+2}{n(n+1)(n+2)}\left[\ln 4\pi-\gamma_E+2\sum_{j=1}^{n}\frac{1}{j}\right]-\frac{3}{2(n+2)}-\frac{1}{n+1}+\frac{3}{2n}\right].$$

These functions, in contrast to Eq. (1.4), are bounded functions of n, and in particular they have no $\ln^2 n$ terms. They are plotted in Fig. 6, where the quantities $\omega_{ab}^{(F,1)}(n)$ obtained from DIS structure functions[2,3] are shown for comparison. The gluon corrections are still negative and small, while the fermion corrections are still rather large, though considerably smaller than those found in Refs. 2 and 3. Due to the absence of the distribution $[\ln(1-z)/(1-z)]_+$ in (4.5) and hence of $\ln^2 n$ terms in (4.6), the expression for $\omega_{q\bar{q}}^{(\phi,1)}(n)$ is almost independent of n for all but the first five moments. The bulk of the remaining contribution arises from the term proportional to π^2. In particular, the π^2 corrections are exactly the same as for Refs. 2 and 3.

It should be noted that the π^2 terms are ultraviolet in nature, and as such should be asymptotically calculable by perturbative QCD. Indeed, were they not, factorization would not make sense. This does not contradict the fact that the same π^2 terms appear in soft-gluon approximations.[2,13] Their presence in the final answer is required by analyticity. For verification of this fact, we must for the most part depend on proofs of factorization which show how all IR contributions are included in the distributions. To give at least one specific example, however, we have shown how the difference between the one-loop vertex correction for spacelike and timelike q^2 may be considered as a UV quantity. This argument is given in the Appendix.

V. $\ln^2 n$ TERMS

The $\ln^2 n$ terms in cross-section moments are usually described as resulting from incomplete cancellation between real and virtual gluons. Their presence in the hard part of the standard factorization[1] does not contradict the factorization theorem because n introduces a new scale in the problem. So long as n is finite, the hard part remains IR finite, even though it grows with n. In the following we first repeat the standard description of the difference between DY and DIS which gives the mismatch in their $\ln^2 n$ terms. We then interpret this difference in terms of a collinear enhancement which is present in DIS but not in DY. We go on to show that, because $\phi_{i,a}(x,Q^2)$ has no

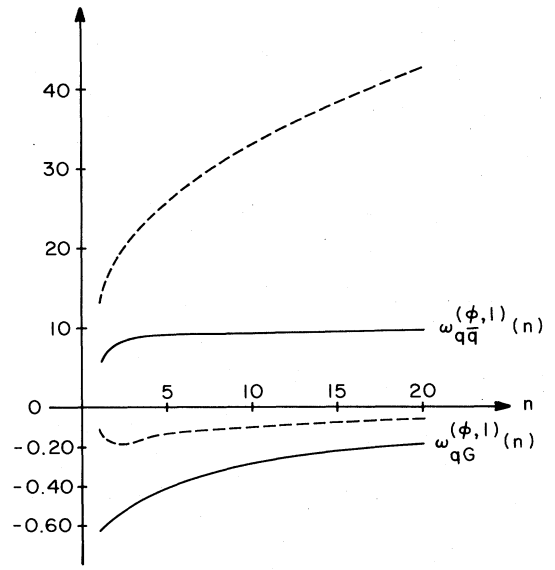

FIG. 6. One-loop corrections to $\omega_{q\bar{q}}^{(\phi)}(n)$ and $\omega_{qG}^{(\phi)}(n)$. Dashed curves represent the corresponding results obtained in Ref. 2. Note different scale for $\omega_{qG}^{(\phi)}$.

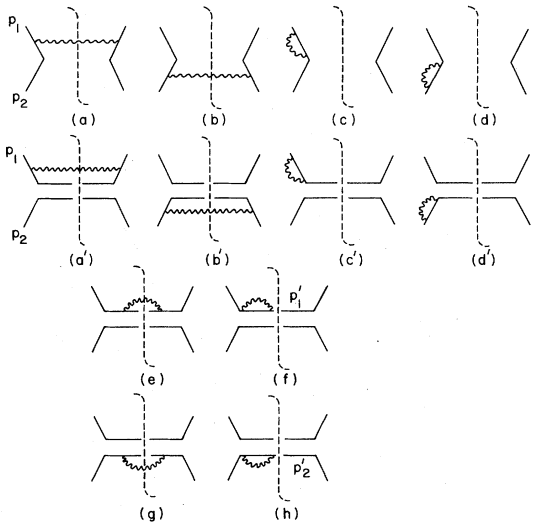

FIG. 7. Double-logarithmic graphs in the axial gauge in DY and DIS.

extraneous enhancements, its leading term has the correct coefficient for factorization. We end with arguments on why these terms exponentiate.

We can explain the coefficients of $\ln^2 n$ terms in both DY and DIS by the integrals[2,3,4]

$$\Delta\frac{4}{3}\frac{\alpha_s}{2\pi}\int_0^1 dx(1+x^2)\frac{x^n-1}{1-x}\int_0^{(\vec{k}_{T,\max})^2}\frac{d\vec{k}_T^{\,2}}{\vec{k}_T^{\,2}}, \quad (5.1)$$

which is the form of the leading contribution to $\ln^2 n$ in both cases. $\Delta=1$ for DY and $\frac{1}{2}$ for DIS. The upper limits are

$$\text{DY: } \vec{k}_T^{\,2}<\frac{1}{4}\frac{(1-x)^2}{x}Q^2,$$
$$\text{DIS: } \vec{k}_T^{\,2}<\frac{1}{4}\frac{(1-x)}{x}Q^2. \quad (5.2)$$

The logarithmic k_T integral thus gives an extra factor of 2 for the $\ln(1-x)$ in DY which, taking into account the value of Δ in (5.1), leads to the $2\ln^2 n$ term in Eq. (1.4) after factorization of the DIS parton densities.

To understand this result in a more physical manner, we refer to the diagrams of Fig. 7. This figure depicts all the axial-gauge one-loop leading-logarithm graphs which contribute to the DY cross section and to $F_1\otimes F_2$, with F_i the DIS structure function of hadron i. The graphs (e) and (g) become double logarithmic only as $x_i=-q^2/2p_i\cdot q\to 1$ for $i=1$ and 2, respectively. The graphs (f) and (h) only contribute at $x_i=1$. Nevertheless, all four graphs contribute to Eq. (5.1) for DIS. To understand why, we consider the frame where $x\equiv -q^2/2p\cdot q=-q^+/p^+$, and $p^+=0$. In this frame, we easily solve for k^- when k_T^2 takes on its maximum value in DIS:

$$k^-=\frac{1}{2}\frac{Q}{(2x)^{1/2}}\gg k^+. \quad (5.3)$$

Thus, at the boundary of phase space in the DIS case k^μ is nearly parallel to $p_i'=q+p_i$, which is becoming lightlike and in the $-\hat{z}$ direction for $x\to 1$. In the DY case, on the other hand, k^+ and k^- are of the same order at the maximum value of $\vec{k}_T^{\,2}$. The resulting collinear divergences from $x\to 1$ in the graphs (e), . . . , (h) cancel in an inclusive cross section, but for large n the real graphs (e) and (g) are suppressed in most of phase space. We then find an incomplete cancellation due to DIS final-state interactions which are not present in DY.

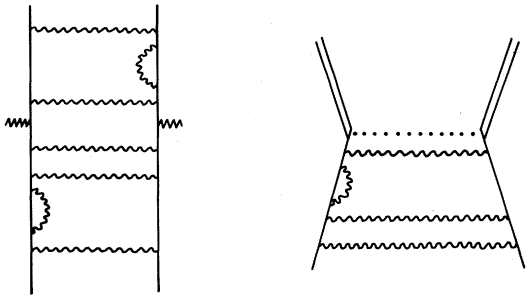

FIG. 8. Ladder structure in DY and ϕ.

In the alternate distribution $\phi_{i,a}$ the situation is somewhat different. There is no kinematic cutoff in the k_T integral. But, because p_i supplies the only external lightlike vector in the diagrams which define ϕ, large k_T are cut off naturally. For example, in calculating Fig. 4(a) we encounter the denominator

$$\frac{1}{\eta\cdot k}=\frac{1}{k^+-k^-}=\frac{1}{(1-x)p^+-\vec{k}_T^{\,2}/2(1-x)p^+}. \quad (5.4)$$

Once we have

$$\vec{k}_T^{\,2}\gg(1-x)^2p^{+2}, \quad (5.5)$$

the integral cuts itself off, so that $(1-x)^2p^{+2}$ acts as an effective kinematic boundary. This is the practical mechanism by which the $\ln^2 n$ terms in ϕ are in agreement with those of DY.

Having discussed the factorization of $\ln^2 n$ terms at one loop, we can extend this result to all leading $\ln^2 n$ terms by appealing to standard reasoning.[6] We used the Feynman gauge above as convenient in the calculation of nonleading terms. For leading logarithms, however, physical gauges are most convenient. Then[6,14] leading logarithms arise from ladder structures of the type shown in Fig. 8 for both DY and the distributions $\phi_{i,a}$. The exponentiation of leading logarithms is then a result of the strong ordering of momenta in the ladders. The result for both $\sigma^{\rm DY}$ and $(\phi_{i,g})^2$ to leading order may be written as

$$\exp\frac{\alpha_s}{\pi}\int^1 dx\frac{x^n-1}{1-x}\int^{(1-x)^2Q^2}\frac{d\vec{k}_T^{\,2}}{\vec{k}_T^{\,2}}, \quad (5.6)$$

where the effective upper limit in the case of ϕ comes about as described above. This result is for the ladder structure without radiative corrections. The effect of including corrections to the ladder structure has been described for DIS in detail in Ref. 15, where it is argued that α_s is replaced by $\alpha_s(k_T^2)$ in Eq. (5.6). We expect that precisely similar things will happen here when nonleading contributions are taken into account using the methods described in Ref. 16.

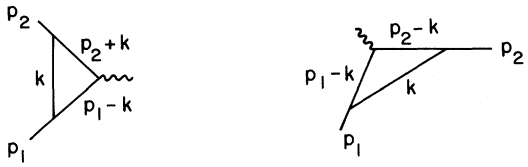

FIG. 9. Vertex corrections in the timelike and spacelike cases.

APPENDIX

In this Appendix, we explicitly verify that the π^2 term occurring in the difference between timelike and spacelike vertex functions may be thought of as a UV contribution.

For simplicity of presentation, we work in a scalar theory. The entire graph is then suppressed by an overall factor of $1/Q^2$, but the structure of the relevant integrals is the same as in a renormalizable theory.

The diagram is shown in Fig. 9, with momentum assignments relevant for spacelike and timelike external "photon." We work with light-cone variables, and choose

$$p_1=\left[\frac{m^2}{2Q},\ Q,\ \vec{0}_T\right],\qquad p_2=\left[Q,\ \frac{m^2}{2Q},\ \vec{0}_T\right]. \tag{A1}$$

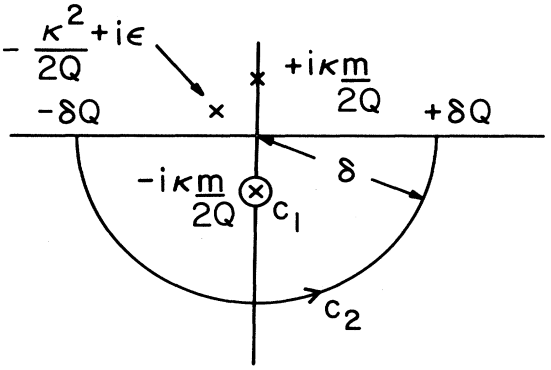

FIG. 10. Analytic structure of the integrand of (A8) in the k^+ plane.

We first evaluate the k^- integral by closing its contour in the upper half-plane in the timelike case, and in the lower half-plane in the spacelike case. The result in both cases may be easily written as the sum of a term from the $(k^2+i\epsilon)^{-1}$ pole and a term from the $[(p_1-k)^2-m^2+i\epsilon]^{-1}$ pole.

The k^2 pole terms, which give the entire double logarithmic contribution, are the same in the spacelike and timelike cases. The spacelike and timelike (p_1-k) pole terms are given by

$$S=-\frac{g^3}{(2\pi)^2m^2}\int_0^\infty d\kappa\,\kappa\int_{m^2/2Q}^{Q}dk^+\frac{k^+-m^2/2Q}{[\kappa^2+4(Q^2/m^2)k^{+2}](\kappa^2-2k^{+2}+2Qk^+-i\epsilon)} \tag{A2}$$

and

$$T=\frac{g^3}{(2\pi)^2m^2}\int_0^\infty d\kappa\,\kappa\int_{-Q}^{m^2/2Q}dk^+\frac{k^+-m^2/2Q}{[\kappa^2+4(Q^2/m^2)k^{+2}](\kappa^2+2k^{+2}+2Qk^+-i\epsilon)}, \tag{A3}$$

respectively, where

$$\kappa^2=\vec{k}_T^{\,2}. \tag{A4}$$

We are interested in the difference $T-S$. To understand where this difference comes from, it is convenient to consider the two regions

$$A:\ |k^+|\le\delta Q,\qquad B:\ |k^+|\ge\delta Q,\ \ \delta\ll 1, \tag{A5}$$

separately.

In region B, we change variables to $-k^+$ in S and find

$$(T-S)_B\approx\frac{g^3}{(2\pi)^2m^2}\int_0^\infty d\kappa\,\kappa\int_{-Q}^{-\delta Q}dk^+\frac{k^+}{[\kappa^2+4(Q^2/m^2)k^{+2}]}\left[\frac{1}{\kappa^2+2k^{+2}+2Qk^+-i\epsilon}-\frac{1}{\kappa^2-2k^{+2}-2Qk^+-i\epsilon}\right]. \tag{A6}$$

This integral is purely imaginary for any $\delta<1$, as may easily be seen by integrating κ first.

In region A, we have

$$|Qk^+|\gg|k^{+2}|, \tag{A7}$$

so we may combine the S and T integrals to get

$$(T-S)_A\approx\frac{g^3}{(2\pi)^2m^2}\int_0^\infty d\kappa\,\kappa\int_{-\delta Q}^{\delta Q}dk^+\frac{k^+-m^2/2Q}{[\kappa^2+4(Q^2/m^2)k^{+2}](\kappa^2+2Qk^+-i\epsilon)}. \tag{A8}$$

The analytic structure of the integrand in the k^+ plane is shown in Fig. 10. There are three poles, at $-\kappa^2/2Q+i\epsilon$, and $\pm i\kappa m/2Q$. We deform the k^+ contour as shown in the figure, into a small circle around $im\kappa/2Q$ (C_I), and semicircle of radius δQ (C_2). C_1 gives a purely imaginary result, as may be seen by evaluating the pole term. The C_2 contour is more interesting to us. Doing the κ integral first we find, to leading power,

$$\frac{g^3}{8(2\pi)^2Q^2}\int_{C_2}\frac{dk^+}{k^+}\ln\left[\frac{2Qk^+}{m^2}\right]=\frac{g^3}{8(2\pi)^2Q^2}\int_{-\pi}^{0}(i\,d\theta)\left[\ln\left[\frac{2Q^2\delta}{m^2}\right]+i\theta\right]=\frac{g^3}{8(2\pi)^2Q^2}\frac{\pi^2}{2}+\text{imaginary}\,. \tag{A9}$$

This is the entire real part of $T-S$. It may be written as

$$\frac{\alpha}{4\pi}\frac{1}{2|q^2|}\pi^2\,,$$

which shows it is of the same form as the difference in the renormalizable theory. We now point out that the contour C_2 is in a UV region for k^+. $|k^+|=\delta Q$, where δ is small but fixed, so it grows with the energy. It is also easy to check that $\kappa=O(\delta Q)$ as well in the region which gives this contribution. Finally, although k^- has been chosen to set the line $(p-k)$ on shell, this pole is at some complex value of k^-, at a distance from the real axis which grows with Q. Thus, we may consider the relevant part of the k^- integral as a circle of order δQ around this complex pole. On this hypercontour in k^-, k^+, and κ, all lines are off-shell by $O(\delta^2Q^2)$, so that we may identify the π^2 correction with a UV region, as claimed.

Finally, we note that because the π^2 term comes from the k^2 pole, it arises from the same UV region when a soft approximation[13] is made by neglecting k^2 compared to $p_i\cdot k$ and simplifying numerators.

[1]H. D. Politzer, Nucl. Phys. B129, 301 (1977); A. H. Mueller Phys. Rep. 73, 237 (1981).

[2]G. Altarelli, R. K. Ellis, and G. Martinelli, Nucl. Phys. B143, 521 (1978); B146, 544(E) (1978); B157, 461 (1979).

[3]J. Kubar-Andre and F. E. Paige, Phys. Rev. D 19, 221 (1979); K. Harada, T. Kaneko, and N. Sakai, Nucl. Phys. B155, 169 (1979); B165, 545(E) (1980); J. Abad and B. Humpert, Phys. Lett. 80B, 286 (1979); B. Humpert and W. L. van Neerven, *ibid.* 84B, 327 (1979).

[4]G. Parisi, Phys. Lett. 90B, 295 (1980).

[5]D. Amati, A. Basseto, M. Ciafaloni, G. Marchesini, and G. Veneziano, Nucl. Phys. B173, 429 (1980); M. Ciafaloni and G. Curci, Phys. Lett. 102B, 352 (1981); C. Curci, M. Greco, and Y. Shrivastava, Nucl. Phys. B159, 451 (1979).

[6]Yu. L. Dokshitzer, D. I. Dyakonov, and S. I Troyan, Phys. Rep. 58, 269 (1980); G. Parisi and R. Petronzio, Nucl. Phys. B154, 427 (1979).

[7]J. C. Collins, D. E. Soper, and G. Sterman, Phys. Lett. 109B, 388 (1982).

[8]J. C. Collins, D. E. Soper, and G. Sterman, Nucl. Phys. B223, 381 (1983).

[9]J. C. Collins, D. E. Soper, and G. Sterman, Phys. Lett. 126B, 275 (1983).

[10]J. C. Collins, D. E. Soper, and G. Sterman, Phys. Lett. 134B, 263 (1984).

[11]G. T. Bodwin, C. Y. Lo, J. D. Stack, and J. D. Sullivan, Phys. Lett. 92B, 337 (1980); P. V. Landshoff and W. J. Stirling, Z. Phys. C 14, 251 (1982); F. Khalafi, *ibid.* 18, 57 (1983).

[12]G. Altarelli and G. Parisi, Nucl. Phys. B126, 298 (1977).

[13]A. P. Contogouris, S. Papadopoulos, and J. P. Ralston, Phys. Rev. D 25, 1280 (1982).

[14]G. Altarelli, Phys. Rep. 81, 1 (1982).

[15]Ciafaloni and Curci (Ref. 5).

[16]J. C. Collins and D. E. Soper, Nucl. Phys. B193, 381 (1981).